J. Fluid Mech. (2025), *vol.* 1009, A2, doi:10.1017/jfm.2025.140

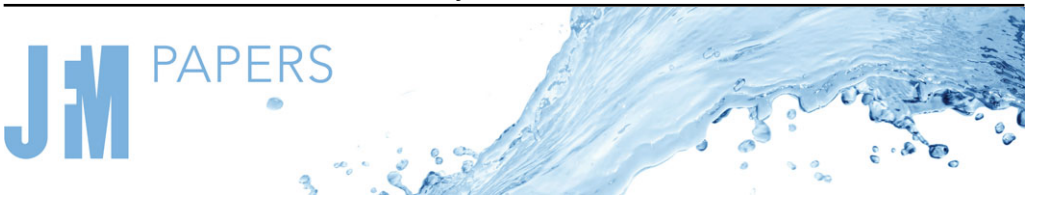

Noise-expansion cascade: an origin of randomness of turbulence

Shijun Liao[1,2] **and Shijie Qin**[2]

[1]State Key Laboratory of Ocean Engineering, Shanghai 200240, PR China

[2]School of Ocean and Civil Engineering, Shanghai Jiao Tong University, Shanghai 200240, PR China

Corresponding author: Shijun Liao, sjliao@sjtu.edu.cn

(Received 1 December 2024; revised 21 January 2025; accepted 26 January 2025)

Randomness is one of the most important characteristics of turbulence, but its origin remains an open question. By means of a 'thought experiment' via several clean numerical experiments based on the Navier–Stokes equations for two-dimensional turbulent Kolmogorov flow, we reveal a new phenomenon, which we call the 'noise-expansion cascade' whereby all micro-level noises/disturbances at different orders of magnitudes in the initial condition of Navier–Stokes equations enlarge consistently, say, one by one like an inverse cascade, to macro level. More importantly, each noise/disturbance input may greatly change the macro-level characteristics and statistics of the resulting turbulence, clearly indicating that micro-level noise/disturbance might have great influence on macro-level characteristics and statistics of turbulence. In addition, the noise-expansion cascade closely connects randomness of micro-level noise/disturbance and macro-level disorder of turbulence, thus revealing an origin of randomness of turbulence. This also highly suggests that unavoidable thermal fluctuations must be considered when simulating turbulence, even if such fluctuations are several orders of magnitudes smaller than other external environmental disturbances. We hope that the 'noise-expansion cascade', as a fundamental property of the Navier–Stokes equations, could greatly deepen our understandings about turbulence, and also be helpful for attacking the fourth millennium problem posed by the Clay Mathematics Institute in 2000.

Key words: turbulence simulation, chaos

1. Introduction

'Turbulence is the last great unsolved problem of classical physics', as pointed out by the Nobel Prize winner Richard Feynman. In particular, randomness is one of the most important characteristics of turbulence (Davidson 2004), but its origin remains an open question until now, to the best of our knowledge.

Today it is widely accepted by the scientific community that turbulent flows can be described mathematically by the Navier–Stokes (NS) equations. The NS equations are so important and fundamental that their solution becomes the fourth millennium problem posed by Clay Mathematics Institute of Cambridge, Massachusetts (2000). In a pioneering paper, Orszag (1970) proposed the 'direct numerical simulations' (DNS) that numerically solved the NS equations without any turbulence mode. Since then, DNS have become a useful tool in fundamental research of turbulence (Rogallo 1981; She, Jackson & Orszag 1990; Nelkin 1992; Coleman & Sandberg 2010; Alexakis *et al*. 2024), and each result given by DNS has been regarded as a 'clean' benchmark solution, because it is widely believed that numerical noise of DNS would not grow to reach the macroscopic level due to fluid viscosity. Coleman & Sandberg (2010) pointed out that DNS have 'the ability to perform fundamental studies of *clean* flows *unaffected* by numerical, modelling and measurement errors' and 'the complete control of the initial and boundary conditions, and each term in the governing equations, also leads to profound advantages over laboratory and field studies'. It should be emphasised here that researchers traditionally focus on 'the initial and boundary conditions' and flow domain of turbulence, but mostly neglect the influence of micro-level noises such as thermal fluctuation and environmental disturbances.

However, turbulence governed by the NS equations should be chaotic, i.e. its spatiotemporal trajectories are very sensitive (i.e. unstable) to the initial conditions (Deissler 1986; Boffetta & Musacchio 2017; Berera & Ho 2018). Recently, Ge, Rolland & Vassilicos (2023) reported that the average uncertainty energy of three-dimensional NS turbulence grows exponentially. A similar phenomenon, sometimes called 'inverse error cascade', was also reported in some previous publications (Aurell *et al*. 1996; Boffetta & Musacchio 2001, 2010; Boffetta & Ecke 2012; Lin, Wang & Liao 2017; Ma *et al*. 2024), and was due to the famous butterfly effect of chaos. Note that the difference in initial condition of these previous publications is at the same order of magnitude. Different from these previous publications, in this paper, we focus on the influence of several micro-level noises/disturbances at quite different orders of magnitudes. Here, the noises/disturbances might be either physical environmental noises (such as those caused by thermal fluctuations) or artificial disturbances. It should be emphasised that, as pointed out by Coleman & Sandberg (2010), 'the profound advantages over laboratory and field studies' of numerical experiment is the 'complete control of the initial and boundary conditions'. Therefore, we can use such kinds of freedom in choice of initial/boundary condition of the NS equations to do some 'thought experiments' so as to deepen our understandings about turbulence. Here, let $f(\boldsymbol{r}) + \Delta_1(\boldsymbol{r}) + \Delta_2(\boldsymbol{r})$ denote an initial condition of the NS equations, where $\boldsymbol{r}$ is a spatial vector, $f(\boldsymbol{r})$ is a function at the macro level, $\Delta_1(\boldsymbol{r})$ is a small disturbance at a micro level, for example at the order 10^{-20} of magnitude, and $\Delta_2(\boldsymbol{r})$ is an even smaller disturbance, for example at the order 10^{-40} of magnitude. Traditionally, it is widely believed that the second disturbance $\Delta_2(\boldsymbol{r})$ could be negligible since it is 20 orders of magnitude smaller than the first disturbance $\Delta_1(\boldsymbol{r})$. Is this traditional viewpoint really correct for turbulent flow governed by NS equations? This is a fundamental problem, which, to the best of our knowledge, is also an open question.

In order to answer the two open questions mentioned above, it is necessary to develop a new kind of numerical algorithm, whose numerical noise must be much smaller than

micro-level physical disturbances and artificial numerical noise throughout a finite but long enough interval of time. In 2009, a method called 'clean numerical simulation' (CNS) was proposed by Liao (2009) for solving problems involving chaos and turbulence, and since then its computational efficiency has been increased, step by step, by several orders of magnitude (Liao & Wang 2014; Lin *et al*. 2017; Hu & Liao 2020; Qin & Liao 2020, 2023*a*,*b*, 2024; Liao & Qin 2022; Liao 2023). Unlike DNS, the CNS algorithm uses multiple precision (Oyanarte 1990) with sufficient significant digits and thus can decrease both the truncation error and round-off error to any given tiny level. Thus numerical noise of CNS can be rigorously negligible throughout a time interval $t \in [0, T_c]$ that is long enough for calculating statistics (Liao 2023), where T_c is called 'the critical predictable time'. The CNS result is therefore much more accurate than its DNS counterpart over a finite but long enough interval of time, so can be used as a clean benchmark solution to check, for the first time, the validity of DNS.

For example, it was found by Qin & Liao (2022) that the DNS result of a two-dimensional (2-D) turbulent Rayleigh–Bénard (RB) convection, which is excited by the thermal fluctuation as an initial condition, quickly departs from the corresponding CNS benchmark solution: the result initially exhibits a non-shearing vortical/roll-like convection, but then it quickly turns into a kind of zonal flow, while the CNS benchmark solution consistently retains the same non-shearing vortical/roll-like convection behaviour over a finite but long enough time interval $t \in [0, T_c]$, where T_c, called 'the critical predictable time', is equal to 500 for the RB convection under consideration. To further confirm this, 2-D turbulent Kolmogorov flow, excited by an initial condition with a kind of spatial symmetry, was solved by DNS and CNS, respectively (Qin *et al*. 2024). It was found that the spatiotemporal trajectory of the CNS benchmark solution retains the same spatial symmetry as the initial condition throughout the whole interval of time [0, 1000]; however, the spatiotemporal trajectory of the corresponding DNS result is the same at the beginning as the CNS benchmark result, but quickly loses the spatial symmetry, clearly indicating that the spatiotemporal trajectory of the 2-D turbulent Kolmogorov flow given by DNS is badly polluted by artificial numerical noise that quickly increases to the same order of magnitude as the exact solution of the NS equations. This clearly illustrated that the 2-D turbulent Kolmogorov flow is a chaotic system in that its spatiotemporal trajectory is rather sensitive to small disturbances caused by artificial numerical noise (Qin *et al.* 2024). More importantly, as illustrated by Qin & Liao (2022) and Qin *et al.* (2024), the DNS result sometimes may deviate greatly from the CNS benchmark solution not only in flow type and/or spatial symmetry of flow field, but also even in statistics. These two successful applications of CNS illustrated that CNS can indeed provide us with the capability to carry out clean numerical experiments that enable us to investigate accurately the evolution and propagation of micro-level noises/disturbances in the initial condition of the NS equations for turbulence. It should be emphasised that this object cannot be realised by DNS whose numerical noise quickly increases to the same order of magnitude as the true solution, as illustrated by Qin & Liao (2022) and Qin *et al.* (2024).

In addition, CNS has been used successfully to attack some rather difficult problems in classical mechanics. For example, the number of periodic orbits of the famous three-body problem, which can be traced back to Newton in 1687, has been increased by several orders of magnitude by means of CNS (Li & Liao 2017; Li, Jing & Liao 2018; Liao, Li & Yang 2022). This is because CNS, unlike other traditional numerical methods, can correctly calculate the essentially chaotic trajectories of the three-body system (Crane 2017; Whyte 2018). The three-body problem highlights the need to determine the precise spatiotemporal trajectory of certain complicated dynamic systems.

In this paper, greatly inspired by spatial symmetry of the CNS benchmark solution (Qin *et al.* 2024) of the 2-D turbulent Kolmogorov flow, we properly conceive/design several clean numerical experiments based on CNS for a 2-D turbulent Kolmogorov flow governed by the NS equations with specially chosen initial conditions that contain terms of different orders of magnitudes and have different spatial symmetries, so as to accurately investigate these terms' propagations, evolutions and macro-scale influences on the turbulence. These clean numerical experiments provide us with rigorous evidence that all noises/disturbances at different orders of magnitudes in the initial condition of the NS equations could enlarge, one by one like an inverse cascade, to a macro level, and moreover, each of them could greatly change the later turbulence characteristics. Based on this interesting phenomenon, we propose a new concept, which we call the 'noise-expansion cascade'. The noise-expansion cascade closely connects the randomness of the initial micro-level noise/disturbance to the later macro-level disorder of turbulence, and thus reveals an origin of randomness of turbulence. In addition, according to the concept of the noise-expansion cascade, unavoidable thermal fluctuations must be considered when simulating turbulence, even if such fluctuations are many orders of magnitudes smaller than other external disturbances.

The paper is structured as follows. Section 2 describes the design of the clean numerical experiments. Section 3 reports the detailed results obtained using the clean numerical experiments, notably the noise-expansion cascade phenomenon. Section 4 discusses the main findings of the work.

2. Clean numerical experiment

Consider the 2-D incompressible Kolmogorov flow (Obukhov 1983; Chandler & Kerswell 2013; Wu *et al.* 2021) in a square domain $[0,\, L]^2$ (with a periodic boundary condition) under Kolmogorov forcing, which is stationary, monochromatic and cosusoidally varying in space, with an integer n_K describing the forcing scale, and χ representing the corresponding forcing amplitude per unit mass of fluid. Using the length scale $L/2\pi$ and the time scale $\sqrt{L/2\pi\chi}$, the non-dimensional NS equation of this 2-D Kolmogorov flow in the form of a stream function reads

$$\frac{\partial}{\partial t}(\nabla^2\psi) + \frac{\partial(\psi,\, \nabla^2\psi)}{\partial(x,\, y)} - \frac{1}{Re}\nabla^4\psi + n_K\cos(n_K y) = 0, \tag{2.1}$$

where

$$Re = \frac{\sqrt{\chi}}{\nu}\left(\frac{L}{2\pi}\right)^{3/2}$$

is the Reynolds number, ν denotes the kinematic viscosity, ψ is the stream function, $x,\, y \in [0,\, 2\pi]$ are horizontal and vertical coordinates, t denotes the time, ∇^2 is the Laplace operator, $\nabla^4 = \nabla^2\nabla^2$, and

$$\frac{\partial(a,\, b)}{\partial(x,\, y)} = \frac{\partial a}{\partial x}\frac{\partial b}{\partial y} - \frac{\partial b}{\partial x}\frac{\partial a}{\partial y}$$

is the Jacobi operator. Note that the stream function ψ always satisfies the periodic boundary condition

$$\psi(x,\, y,\, t) = \psi(x + 2\pi,\, y,\, t) = \psi(x,\, y + 2\pi,\, t). \tag{2.2}$$

In order to have a relatively strong state of turbulent flow, we choose $n_K = 16$ and $Re = 2000$ for all cases considered in this paper.

Let us consider the following three different initial conditions:

$$\psi(x, y, 0) = -\tfrac{1}{2}\big[\cos(x+y) + \cos(x-y)\big], \tag{2.3}$$

$$\psi(x, y, 0) = -\tfrac{1}{2}\big[\cos(x+y) + \cos(x-y)\big] + \delta' \sin(x+y), \tag{2.4}$$

$$\psi(x, y, 0) = -\tfrac{1}{2}\big[\cos(x+y) + \cos(x-y)\big] + \delta' \sin(x+y) + \delta'' \sin(x+2y), \tag{2.5}$$

where δ' and δ'' are constants, corresponding to a Kolmogorov flow with different spatial symmetry, as mentioned below.

Note that the initial condition (2.3) has the spatial symmetry

$$\begin{cases} \text{rotation} & \psi(x, y, t) = \psi(2\pi - x, 2\pi - y, t), \\ \text{translation} & \psi(x, y, t) = \psi(x + \pi, y + \pi, t), \end{cases} \tag{2.6}$$

at $t = 0$. Here, we emphasise that Qin *et al.* (2024) solved the 2-D turbulent Kolmogorov flow governed by (2.1) and (2.2) subject to the initial condition (2.3) in the case $n_K = 4$ and $Re = 40$ by means of DNS and CNS. They found that the spatiotemporal trajectory given by DNS agrees well with the CNS benchmark solution from the beginning, and retains the spatial symmetry (2.6) until $t \approx 120$ when the DNS result completely loses spatial symmetry, unlike the CNS benchmark solution, which retains the spatial symmetry (2.6) throughout the whole time interval $t \in [0, 1500]$, clearly indicating that the spatiotemporal trajectory given by DNS is badly polluted by artificial numerical noise when $t \geqslant 120$. So it is impossible to obtain rigorous, accurate prediction of the evolution and propagation of micro-level disturbance by DNS. Therefore, we have to give up DNS in this paper, but use CNS instead. Importantly, Qin *et al.* (2024) revealed the important fact that the 2-D Kolmogorov turbulent flow given by CNS retains the same spatial symmetry as its initial condition; we will use this fact to do a thought experiment via several clean numerical experiments based on CNS, given that the same findings about spatial symmetry should apply qualitatively for the case $n_K = 16$ and $Re = 2000$ considered in this paper.

The CNS algorithm is now described briefly. First, to decrease the spatial truncation error to a small enough level, as in DNS, we discretise the spatial domain of the flow field by a uniform mesh $N^2 = 1024^2$, and adopt the Fourier pseudo-spectral method for spatial approximation with the 3/2 rule for dealiasing. In this way, the corresponding spatial resolution is fine enough for the considered Kolmogorov flow: the grid spacing is less than the average Kolmogorov scale and enstrophy dissipative scale, as mentioned by Pope (2001) and Boffetta & Ecke (2012). In addition, in order to decrease the temporal truncation error to a small enough level, unlike DNS, we use the 140th-order (i.e. $M = 140$) Taylor expansion with a time step $\Delta t = 10^{-3}$. Furthermore, different from DNS, we use multiple precision with 260 significant digits (i.e. $N_s = 260$) for all physical/numerical variables and parameters, so as to decrease the round-off error to a small enough level. In addition, the self-adaptive CNS strategy (Qin & Liao 2023*b*) and parallel computing are adopted to dramatically increase the computational efficiency of the CNS algorithm. In particular, another CNS result is given by the same CNS algorithm but with even smaller numerical noise (i.e. using even larger M and/or N_s than those mentioned above), which confirms (by comparison) that the numerical noise of the former CNS result (say, given by $N = 1024$, $M = 140$ and $N_s = 260$) remains rigorously negligible throughout the whole time interval $t \in [0, 300]$ so that it can be used as a clean benchmark solution. For further details, refer to Qin *et al.* (2024) and Liao (2023). Note that the related code of CNS and some movies can be downloaded via GitHub (https://github.com/sjtu-liao/2D-Kolmogorov-turbulence).

3. Results of clean numerical experiments

Our clean numerical experiments based on CNS comprise two stages.

(i) In the first stage, we set $\delta' = O(1)$ and $\delta'' = O(1)$ in (2.4) and (2.5), then confirm by means of CNS that the 2-D turbulent Kolmogorov flow subject to the initial condition (2.3) or (2.4) always retains the same spatial symmetry as its corresponding initial condition, but the turbulent flow subject to the initial condition (2.5) has no spatial symmetry at all.

(ii) In the second stage, we set $\delta' = 10^{-20}$ and $\delta'' = 10^{-40}$ in (2.4) and (2.5), then carry out the corresponding clean numerical experiments by means of CNS. We name the CNS results subject to the three different initial conditions (2.3), (2.4) and (2.5) as Flow CNS, Flow CNS$'$ and Flow CNS$''$, respectively. The so-called noise-expansion cascade phenomenon is revealed by comparing the evolutions of spatial symmetry of these three turbulent flows.

Details of our clean numerical experiments based on CNS are described below.

3.1. *Spatial symmetry under different initial conditions*

Equations (2.1) and (2.2) subject to the initial condition (2.3) in the case $Re = 2000$ and $n_K = 16$ are solved numerically by means of CNS. It is found that this CNS flow always retains the same spatial symmetry (2.6) throughout the whole time interval $t \in [0, 300]$, exactly as the initial condition (2.3). This accords with the finding about the spatial symmetry of the 2-D Kolmogorov turbulent flow obtained by Qin *et al.* (2024) using CNS for the different case $Re = 40$ and $n_K = 4$. According to the governing equation (2.1), the periodic boundary condition (2.2), the initial condition (2.3) and the spatial symmetry (2.6), the corresponding solution should be in series form as

$$\psi(x, y, t) = \sum_{m+n=2r} a_{m,n}(t)\cos(mx + ny) + \sum_{m-n=2q} b_{m,n}(t)\cos(mx - ny),$$

where $a_{m,n}(t)$, $b_{m,n}(t)$ are unknown time-dependent coefficients, and $m \geqslant 0$, $n \geqslant 0$, $r > 0$, q are integers. Thus the vorticity $\omega = \nabla^2\psi$ of the flow field naturally retains the same spatial symmetry throughout the time interval $t \in [0, 300]$, i.e.

$$\begin{cases} \text{rotation} & \omega(x, y, t) = \omega(2\pi - x, 2\pi - y, t), \\ \text{translation} & \omega(x, y, t) = \omega(x + \pi, y + \pi, t). \end{cases} \tag{3.1}$$

Note that the initial condition (2.4) in the case $\delta' = 1$ has spatial symmetry in translation, say,

$$\psi(x, y, t) = \psi(x + \pi, y + \pi, t), \quad \omega(x, y, t) = \omega(x + \pi, y + \pi, t) \tag{3.2}$$

for $t = 0$ here. Similarly, it is found that the corresponding CNS solution governed by (2.1) and (2.2) subject to the initial condition (2.4) with $\delta' = 1$ always retains the same spatial symmetry (3.2) throughout the whole time interval $t \in [0, 300]$. In addition, it is further found that the same spatial symmetry (3.2) is obtained as long as δ' is a constant at a macro-level $O(1)$, such as $\delta' = 2, -3, \pi$, and so on. It should be emphasised that the initial condition (2.3) and the spatial symmetry (2.6) involve two kinds of spatial symmetry, i.e. rotation and translation, but the initial condition (2.4) in the case $\delta' = O(1)$ and the spatial symmetry (3.2) have only one, i.e. translation.

Note that the initial condition (2.5) in the case $\delta' = 1$ and $\delta'' = 1$ has no spatial symmetry, due to its third term $\sin(x + 2y)$. In a similar way, it is found that the

corresponding CNS solution indeed has no spatial symmetry throughout the whole time interval $t \in [0, 300]$. The same conclusion about the spatial symmetry is obtained as long as δ' and δ'' are constants at a macro-level $O(1)$, such as δ' δ', $\delta'' = 2, -3, \pi$, and so on.

Using the aforementioned findings from clean numerical experiments based on CNS, we discover the so-called noise-expansion cascade phenomenon by undertaking the clean numerical experiments described below.

3.2. *Discovery of the noise-expansion cascade*

In the second stage of our clean numerical experiments based on CNS, we hereafter choose $\delta' = 10^{-20}$ and $\delta'' = 10^{-40}$ in the initial conditions (2.4) and (2.5), corresponding to two micro-level disturbances $10^{-20}\sin(x + y)$ and $10^{-40}\sin(x + 2y)$, where the second is 20 orders of magnitude smaller than the first. Thus the initial conditions (2.4) and (2.5) become hereafter

$$\psi(x, y, 0) = -\tfrac{1}{2}\big[\cos(x + y) + \cos(x - y)\big] + 10^{-20}\sin(x + y), \tag{3.3}$$

$$\psi(x, y, 0) = -\tfrac{1}{2}\big[\cos(x + y) + \cos(x - y)\big] + 10^{-20}\sin(x + y) + 10^{-40}\sin(x + 2y), \tag{3.4}$$

respectively. In other words, (2.1) and (2.2) in the case $Re = 2000$ and $n_K = 16$ are solved by means of CNS in the time interval $t \in [0, 300]$, subject to initial condition (2.3), (3.3) or (3.4), whose clean numerical simulations are called hereafter Flow CNS, Flow CNS′ and Flow CNS″, for the sake of simplicity. Note that according to the three different initial conditions (2.3), (3.3) and (3.4), Flow CNS′ is equal to Flow CNS plus $\delta_1(x, y, t)$, and Flow CNS″ is equal to Flow CNS′ plus $\delta_2(x, y, t)$, where $\delta_1(x, y, t)$ and $\delta_2(x, y, t)$ denote the spatiotemporal evolution of the first disturbance $10^{-20}\sin(x + y)$ and the second disturbance $10^{-40}\sin(x + 2y)$ in the initial conditions (3.3) and (3.4), respectively.

Due to the butterfly effect of chaos, a micro-level disturbance of a chaotic system grows exponentially to the macro level (Deissler 1986; Aurell *et al.* 1996; Boffetta & Musacchio 2001; Boffetta & Ecke 2012; Boffetta & Musacchio 2017; Berera & Ho 2018; Ge *et al.* 2023; Ma *et al.* 2024). Logically, the smaller the disturbance, the longer the time it requires to reach the macro level. According to Qin *et al.* (2024), the two turbulent Kolmogorov flows under consideration are chaotic systems. Therefore, $\delta_2(x, y, t)$, corresponding to the second disturbance $10^{-40}\sin(x + 2y)$, requires more time to reach the macro level than $\delta_1(x, y, t)$, corresponding to the first disturbance $10^{-20}\sin(x + 2y)$. According to our previous clean numerical experiments mentioned in § 3.1, when both $\delta_1(x, y, t)$ and $\delta_2(x, y, t)$ are negligible, Flow CNS′ and Flow CNS″ should have the same spatial symmetry (2.6) as the initial condition (2.3). However, when $\delta_1(x, y, t)$ corresponding to the first disturbance enlarges to a macro-level $O(1)$ but $\delta_2(x, y, t)$ is still at a micro level and thus negligible, the corresponding Flow CNS′ and Flow CNS″ should have the same spatial symmetry (3.2) as the initial condition (2.4) when $\delta' = O(1)$. In addition, when both $\delta_1(x, y, t)$ and $\delta_2(x, y, t)$ enlarge to a macro-level $O(1)$, the corresponding Flow CNS″ should have no spatial symmetry at all, just like 2-D turbulent Kolmogorov flow subject to the initial condition (2.5) when $\delta' = O(1)$ and $\delta'' = O(1)$. Thus by comparing the spatial symmetry of Flow CNS, Flow CNS′ and Flow CNS″ given by our clean numerical experiments, we can find out when the evolution $\delta_1(x, y, t)$, corresponding to the first disturbance $10^{-20}\sin(x + y)$, and the evolution $\delta_2(x, y, t)$, corresponding to the second disturbance $10^{-40}\sin(x + 2y)$, enlarge to macro-level $O(1)$.

As shown in figure 1, the vorticity field $\omega(x, y, t)$ of Flow CNS, subject to the initial condition (2.3), is compared with that of Flow CNS′, subject to the initial condition (3.3).

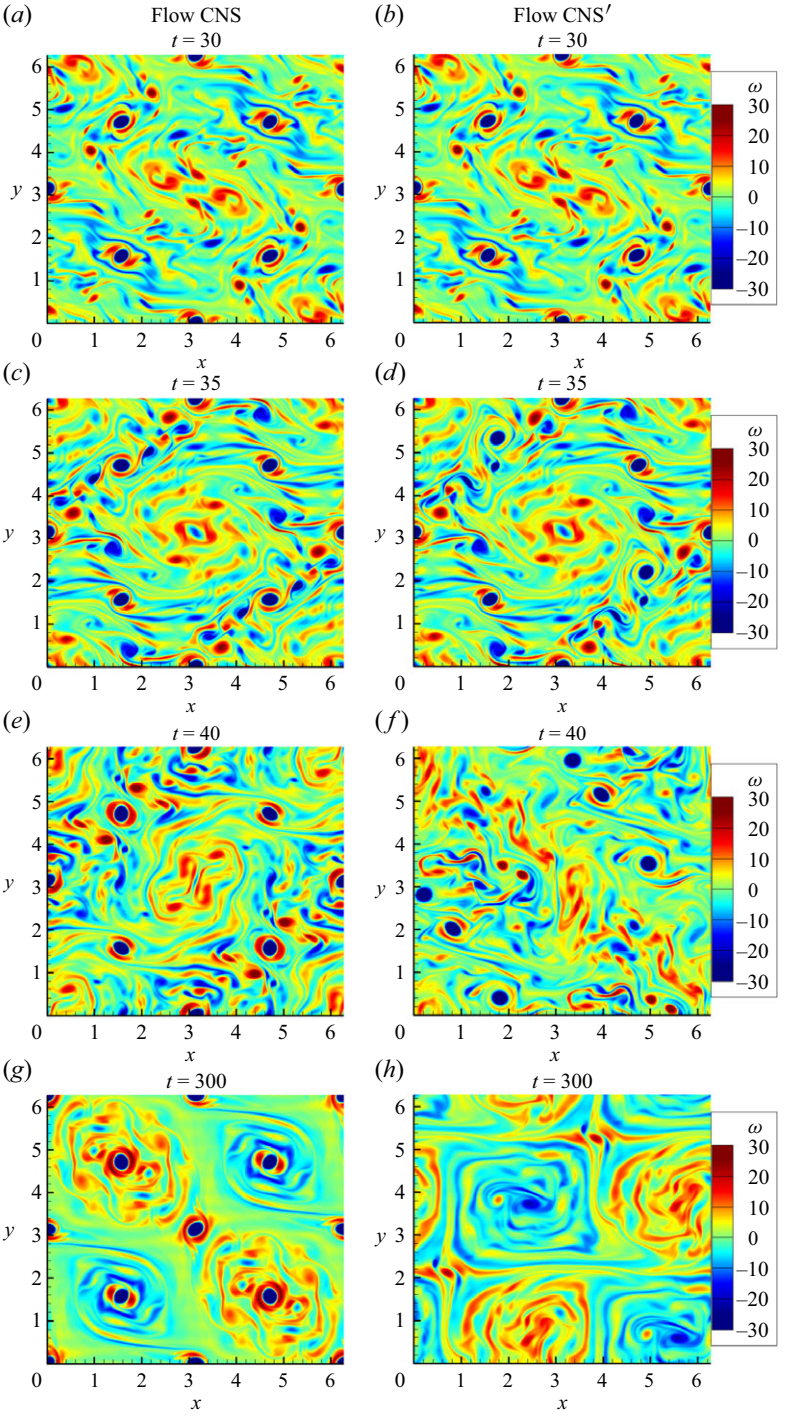

Figure 1. Vorticity fields $\omega(x, y)$ of the 2-D turbulent Kolmogorov flow governed by (2.1) and (2.2) for $n_K = 16$ and $Re = 2000$ given by CNS, subject to either the initial condition (2.3) (left, Flow CNS) or (3.3) (right, Flow CNS′), at different times: (*a*,*b*) $t = 30$, (*c*,*d*) $t = 35$, (*e*,*f*) $t = 40$ and (*g*,*h*) $t = 300$. See supplementary movie 1 for the whole evolution process of vorticity field, which can be downloaded via GitHub (https://github.com/sjtu-liao/2D-Kolmogorov-turbulence).

Note that Flow CNS retains the spatial symmetry (3.1) of vorticity throughout the whole time interval $t \in [0, 300]$. Obviously, the term $10^{-20}\sin(x+y)$ in the initial condition (3.3) can be regarded as a micro-level disturbance added to the initial condition (2.3), since it is 20 orders of magnitude smaller. Certainly, it takes some time for this tiny disturbance $10^{-20}\sin(x+y)$ to be enlarged to a macro-level $O(1)$. Indeed, Flow CNS$'$ appears the same as Flow CNS from the beginning, for example at $t = 30$ as shown in figures 1(*a*) and 1(*b*), when $\delta_1(x, y, t)$ corresponding to the tiny disturbance $10^{-20}\sin(x+y)$ of the initial condition (3.3) has not been increased to macro level, as shown in figures 2(*a–e*), so that both Flow CNS and Flow CNS$'$ agree well and retain the same spatial symmetry (3.1) of vorticity. It is found that the vorticity of Flow CNS$'$ deviates from the spatial symmetry (3.1) obviously at $t \approx 35$, and thereafter loses the spatial symmetry (3.1) but retains the spatial symmetry (3.2) throughout the time interval $t \in [35, 300]$ instead, as shown in figures 1(*c–h*). Note that the term $\sin(x+y)$ of the initial condition (3.3) implies the spatial symmetry of translation but no spatial symmetry of rotation since $\sin(x+y) = \sin(\pi + x + \pi + y)$ but $\sin(x+y) \neq \sin(2\pi - x + 2\pi - y)$. The explanation is provided by considering figure 2: $\delta_1(x, y, t)$ corresponding to the disturbance $10^{-20}\sin(x+y)$ in the initial condition (3.3), which increases from a micro level, step by step, to a macro level at $t \approx 35$, remains the same spatial symmetry (3.2) throughout the whole time interval $t \in [0, 300]$ so that it destroys the spatial symmetry (3.1) and triggers the transition of the spatial symmetry from (3.1) to (3.2) at $t \approx 35$ when it reaches a macro-level $O(1)$. This provides us with rigorous evidence that a very small disturbance $10^{-20}\sin(x+y)$ to the initial condition (3.3) indeed increases to the same order of magnitude as the exact solution of the NS equations at $t \approx 35$, which destroys the spatial symmetry (3.1) and triggers the transition of the spatial symmetry from (3.1) to (3.2).

Figure 3 compares the vorticity field $\omega(x, y, t)$ of Flow CNS$'$, subject to the initial condition (3.3), with that of Flow CNS$''$, subject to the initial condition (3.4). Traditionally, compared with the first disturbance $10^{-20}\sin(x+y)$ in the initial condition (3.4), the second disturbance $10^{-40}\sin(x+2y)$ could be neglected completely, since it is 20 orders of magnitude smaller. However, this traditional viewpoint is in fact wrong: Flow CNS$''$ looks the same as Flow CNS from the beginning until $t \approx 35$, when it loses the spatial symmetry (3.1) but has the new spatial symmetry (3.2) instead, indicating that $\delta_1(x, y, t)$ corresponding to the first disturbance $10^{-20}\sin(x+y)$ increases to macro-level $O(1)$ and thus triggers the transition of the spatial symmetry from (3.1) to (3.2). More importantly, it is found that Flow CNS$''$ appears the same as Flow CNS$'$ from the beginning, for example at $t \approx 88$ as shown in figures 3(*a*) and 3(*b*), until $t \approx 93$, when it loses the spatial symmetry (3.2), as shown in figures 3(*c*) and 3(*d*). Note that Flow CNS$''$ completely loses spatial symmetry after $t \geqslant 98$, as shown in figures 3(*e–h*), clearly indicating that the evolution $\delta_2(x, y, t)$, corresponding to the second micro-level disturbance $10^{-40}\sin(x+2y)$, must increase to a macro-level $O(1)$, and finally destroys the spatial symmetry. Note that the term $\sin(x+2y)$ has no spatial symmetry in rotation and translation, since $\sin(x+2y) \neq \sin(2\pi - x + 4\pi - 2y)$ and $\sin(x+2y) \neq \sin(\pi + x + 2\pi + 2y)$. So the reason is very clear from figure 4: $\delta_2(x, y, t)$, corresponding to the second disturbance $10^{-40}\sin(x+2y)$ in the initial condition (3.4), increases from a micro level, step by step, to a macro level at $t \approx 93$, which has no spatial symmetry throughout the whole time interval $t \in [0, 300]$ so that it destroys the spatial symmetry (3.2) at $t \approx 93$ when it reaches a macro-level $O(1)$.

Let us focus on the initial condition (3.4): the second disturbance $10^{-40}\sin(x+2y)$ is 20 orders of magnitude smaller than the first disturbance $10^{-20}\sin(x+y)$. From the traditional viewpoint, the second disturbance should be negligible compared with the first one. However, on the contrary, both the first disturbance $10^{-20}\sin(x+y)$ and the second

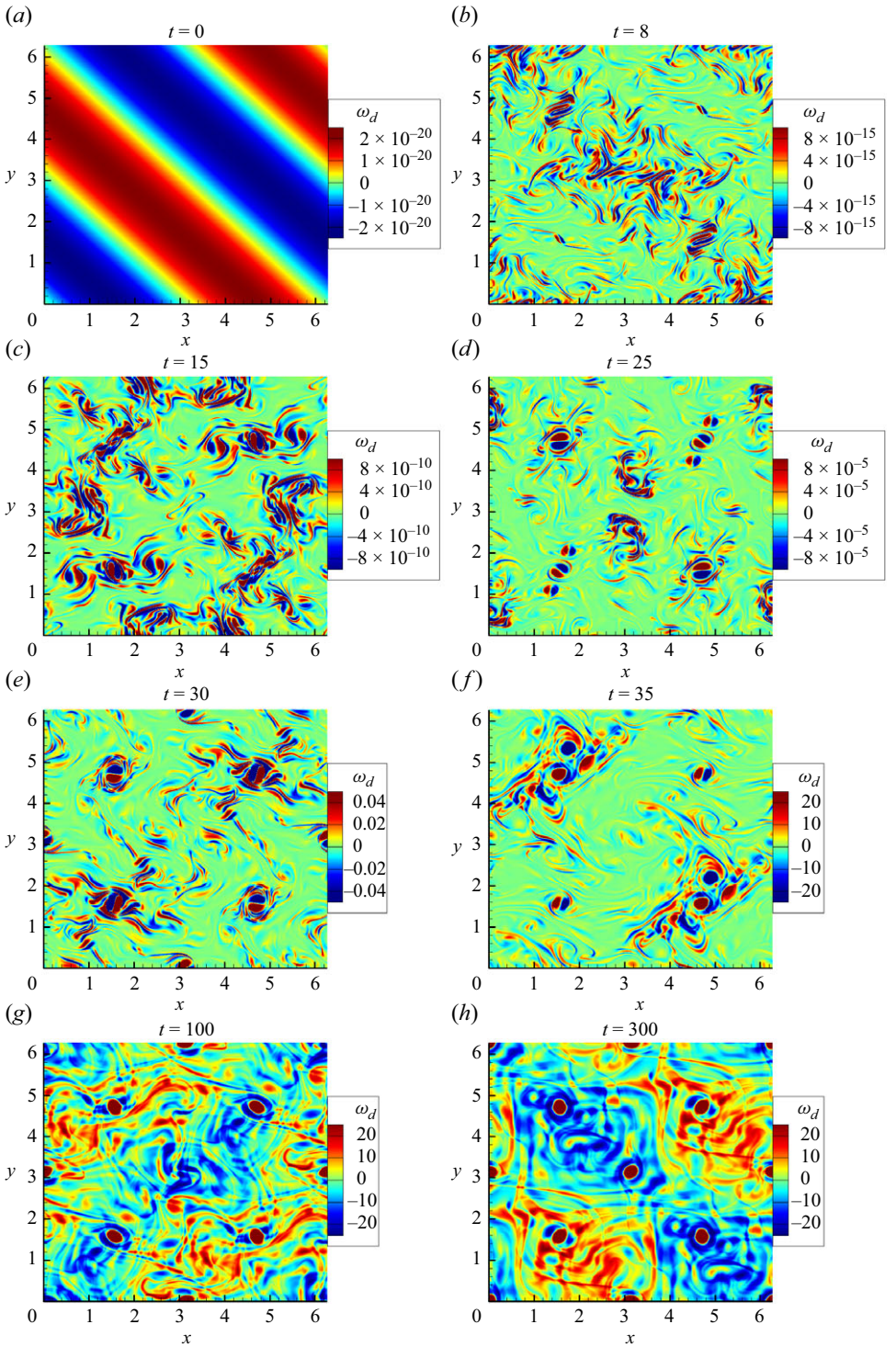

Figure 2. Vorticity fields of the evolution $\delta_1(x, y, t)$, corresponding to the first disturbance $10^{-20}\sin(x + y)$ in the initial condition (3.3) of 2-D turbulent Kolmogorov flow governed by (2.1) and (2.2) for $n_K = 16$ and $Re = 2000$ given by CNS, at the different times (*a*) $t = 0$, (*b*) $t = 8$, (*c*) $t = 15$, (*d*) $t = 25$, (*e*) $t = 30$, (*f*) $t = 35$, (*g*) $t = 100$ and (*h*) $t = 300$.

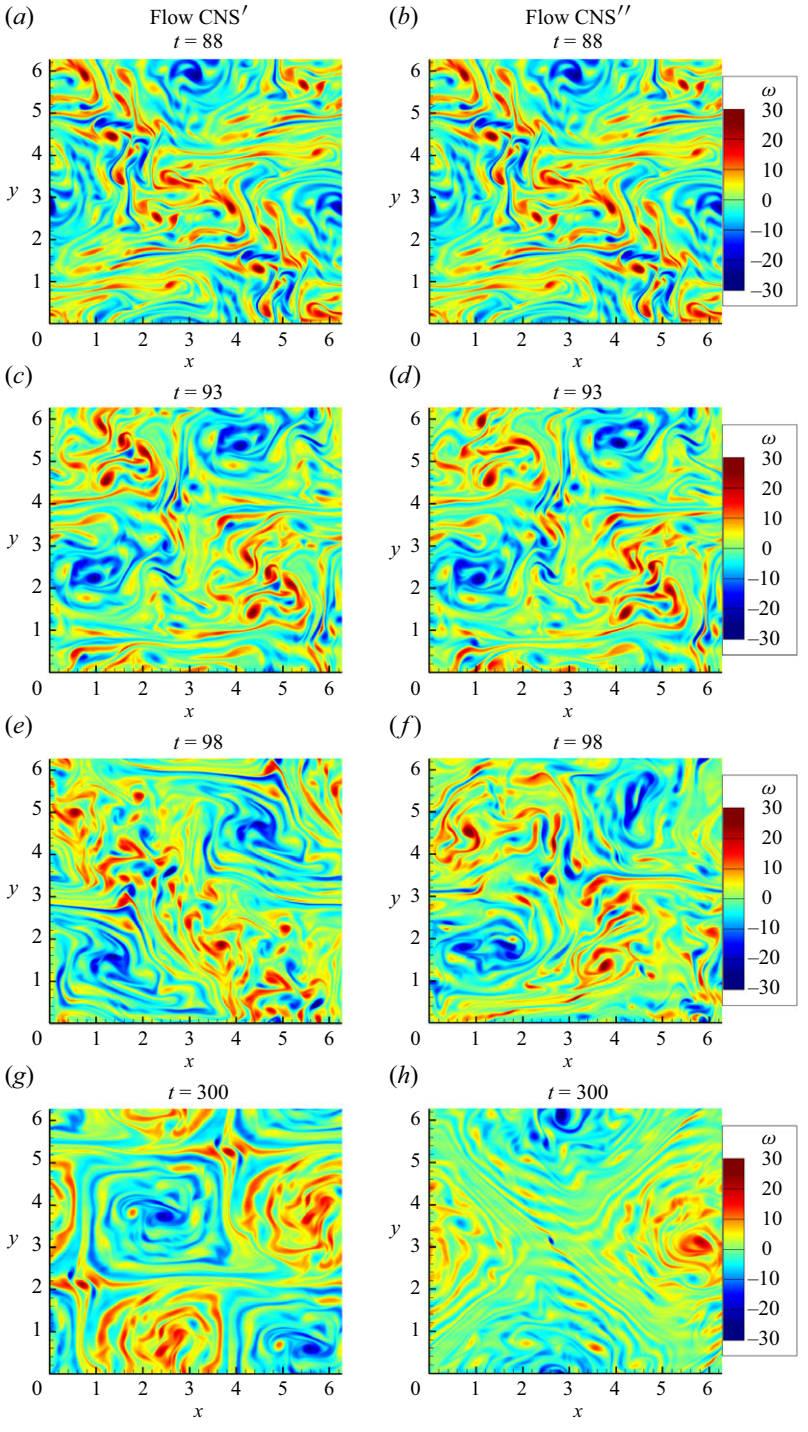

Figure 3. Vorticity fields $\omega(x, y)$ of the 2-D turbulent Kolmogorov flow governed by (2.1) and (2.2) for $n_K = 16$ and $Re = 2000$ given by CNS, subject to either the initial condition (3.3) (left, Flow CNS′) or (3.4) (right, Flow CNS″), at different times: (*a*,*b*) $t = 88$, (*c*,*d*) $t = 93$, (*e*,*f*) $t = 98$ and (*g*,*h*) $t = 300$. See supplementary movie 2 for the whole evolution process, which can be downloaded via GitHub (https://github.com/sjtu-liao/2D-Kolmogorov-turbulence).

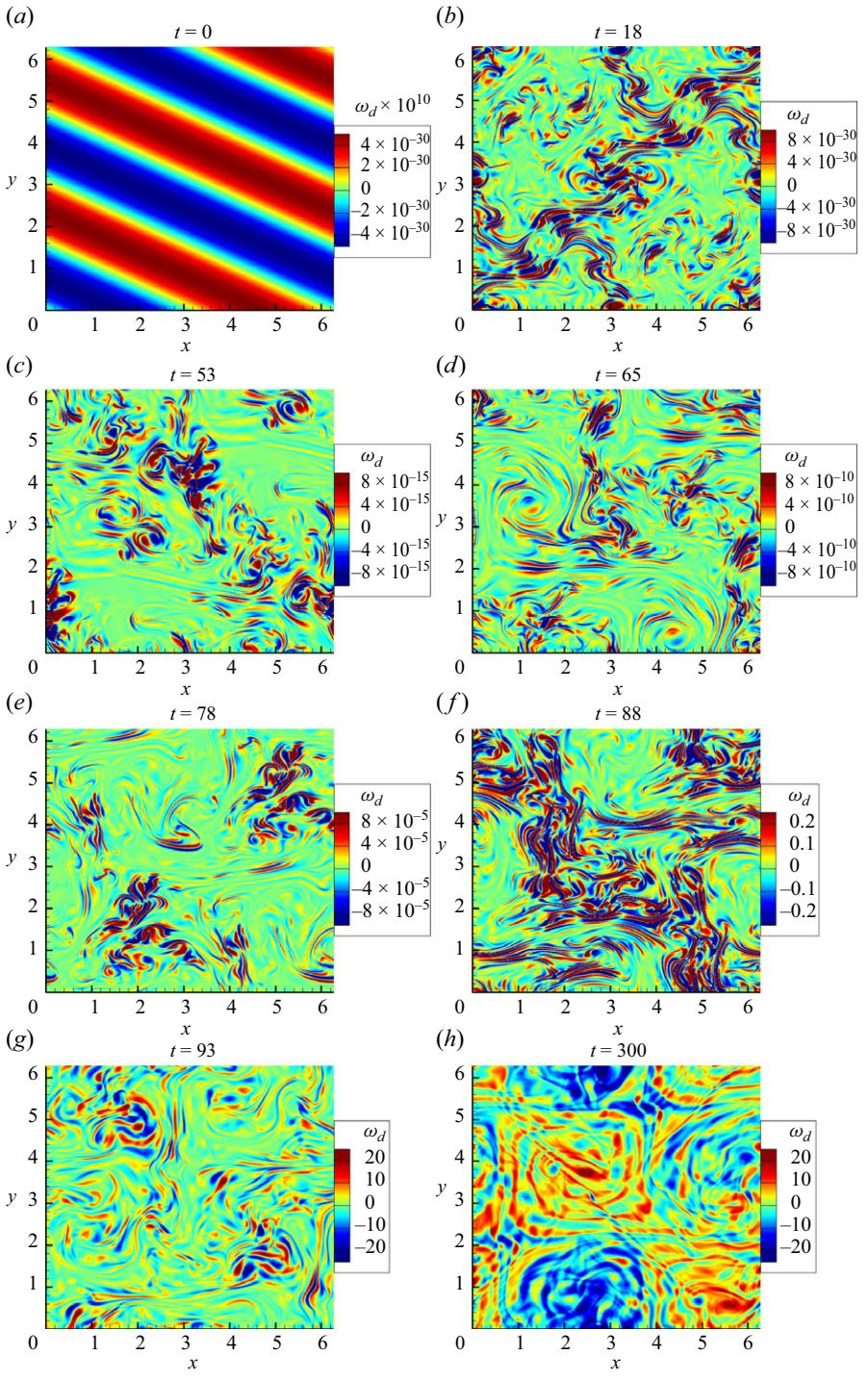

Figure 4. Vorticity fields of the evolution $\delta_2(x, y, t)$, corresponding to the second disturbance $10^{-40}\sin(x + 2y)$ in the initial condition (3.4) of 2-D turbulent Kolmogorov flow governed by (2.1) and (2.2) for $n_K = 16$ and $Re = 2000$ given by CNS, at the different times (*a*) $t = 0$, (*b*) $t = 18$, (*c*) $t = 53$, (*d*) $t = 65$, (*e*) $t = 78$, (*f*) $t = 88$, (*g*) $t = 93$ and (*h*) $t = 300$.

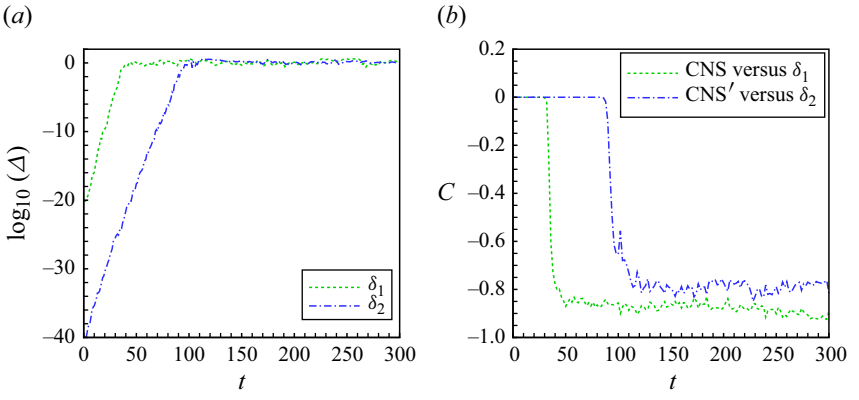

Figure 5. Time histories of (*a*) $\Delta = \sqrt{\langle \delta_i^2 \rangle_A}$ with $i = 1, 2$, where $\delta_1(x, y, t)$ denotes the evolution of the first disturbance (green dashed line) and $\delta_2(x, y, t)$ is the evolution of the second disturbance (blue dash-dotted line) of the initial condition (3.4), and (*b*) the normalised correlation coefficient $C(t)$ of vorticity of Flow CNS versus $\delta_1(x, y, t)$ (green dashed line) as well as that of Flow CNS′ versus $\delta_2(x, y, t)$ (blue dash-dotted line), for the 2-D turbulent Kolmogorov flow governed by (2.1) and (2.2) in the case $n_K = 16$ and $Re = 2000$ subject to the initial condition (3.4).

disturbance $10^{-40}\sin(x + 2y)$ to the initial condition (3.4) enlarge separately, one by one in an inverse cascade, to macro-level $O(1)$: first the former triggers the transformation of the spatial symmetry from (3.1) to (3.2) at $t \approx 35$, then the latter totally destroys the spatial symmetry of the 2-D turbulent Kolmogorov flow at $t \approx 93$. This is very clear from figure 2 for the evolution $\delta_1(x, y, t)$ of the first disturbance $10^{-20}\sin(x + y)$, and figure 4 for the evolution $\delta_2(x, y, t)$ of the second disturbance $10^{-40}\sin(x + 2y)$ of the initial condition (3.4).

Figure 2 shows that the vorticity field caused by $\delta_1(x, y, t)$ corresponding to the first disturbance $10^{-20}\sin(x + y)$ increases from a micro-order $O(10^{-20})$ of magnitude at $t = 0$, step by step, to the order $O(10^{-15})$ at $t = 8$, $O(10^{-10})$ at $t = 15$, $O(10^{-5})$ at $t = 25$, $O(10^{-2})$ at $t = 30$, until a macro-order $O(10)$ at $t = 35$. Figure 4 shows that the vorticity field caused by $\delta_2(x, y, t)$ corresponding to the second disturbance $10^{-40}\sin(x + 2y)$ increases from a micro-order $O(10^{-40})$ of magnitude at $t = 0$, step by step, to the order $O(10^{-30})$ at $t = 18$, $O(10^{-15})$ at $t = 53$, $O(10^{-10})$ at $t = 65$, $O(10^{-5})$ at $t = 78$, $O(10^{-1})$ at $t = 88$, until a macro-order $O(10)$ at $t = 93$. All of these at different orders of magnitude often coexist with a macroscopic flow field.

We write $\Delta = \sqrt{\langle \delta_i^2 \rangle_A}$ with $i = 1, 2$, where $\delta_1(x, y, t)$ and $\delta_2(x, y, t)$ denote the evolutions of the first disturbance $10^{-20}\sin(x + y)$ and the second disturbance $10^{-40}\sin(x + 2y)$ to the initial condition (3.4), respectively, and $\langle\,\rangle_A$ is an operator of statistics defined in Appendix A. As shown in figure 5(*a*), $\sqrt{\langle \delta_1^2 \rangle_A}$ expands exponentially until $t \approx 35$, when it reaches a macro level, i.e. $\sqrt{\langle \delta_1^2 \rangle_A} \sim O(1)$. Similarly, $\sqrt{\langle \delta_2^2 \rangle_A}$ expands exponentially until $t \approx 93$, when it is at a macro level, i.e. $\sqrt{\langle \delta_2^2 \rangle_A} \sim O(1)$. As mentioned before, Flow CNS′ is equal to Flow CNS plus $\delta_1(x, y, t)$, and Flow CNS″ is equal to Flow CNS′ plus $\delta_2(x, y, t)$. As shown in figure 5(*b*), the normalised correlation coefficient of vorticity of Flow CNS versus δ_1 is very small from the beginning to $t \approx 32$, indicating that there is no correlation between them because $\delta_1(x, y, t)$ is negligible compared to Flow CNS, until $t \approx 35$, when their correlation suddenly becomes strong, indicating that

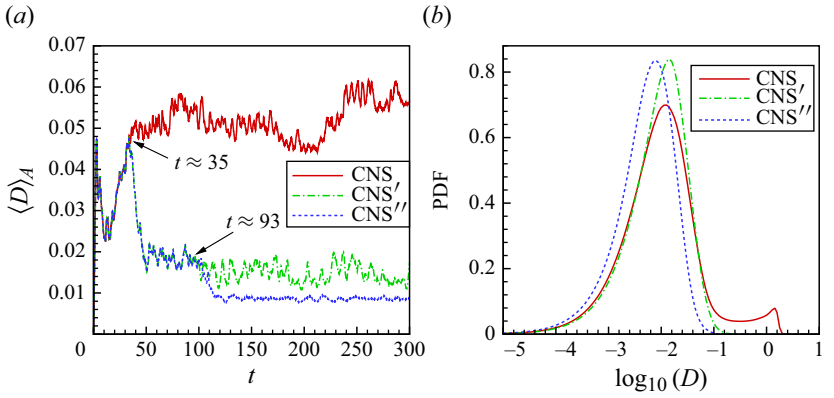

Figure 6. Comparisons of (a) time histories of the spatially averaged kinetic energy dissipation rate $\langle D\rangle_A$ and (b) the probability density function (PDF) of the kinetic energy dissipation $D(x, y, t)$ of the 2-D turbulent Kolmogorov flow, governed by (2.1) and (2.2) for $n_K = 16$ and $Re = 2000$, given by Flow CNS subject to the initial condition (2.3) (red solid line), Flow CNS′ subject to the initial condition (3.3) (green dash-dotted line), and Flow CNS″ subject to the initial condition (3.4) (blue dashed line).

$\delta_1(x, y, t)$ is at the same order of magnitude as Flow CNS and thus is not negligible thereafter. Similarly, the normalised correlation coefficient of vorticity of Flow CNS′ versus $\delta_2(x, y, t)$ is very small from the beginning to $t \approx 90$, indicatingthat there is no correlation between them because $\delta_2(x, y, t)$ is negligible compared to Flow CNS′, until $t \approx 93$, when their correlation suddenly becomes strong, indicating that $\delta_2(x, y, t)$ is at the same order of magnitude as Flow CNS′ and thus is not negligible thereafter.

The foregoing provides rigorous evidence that all disturbances at different orders of magnitude to the initial condition of the NS equations increase separately, say, one by one like an inverse cascade, to macro level, with each capable of completely altering the characteristics (such as the vorticity spatial symmetry) of the turbulent flow considered in this paper. Based on this very interesting phenomenon revealed by our clean numerical experiments mentioned above, we propose a new concept, which we call the 'noise-expansion cascade', that closely connects the randomness of micro-level noises/disturbances to the macro-level disorder of turbulence.

3.3. *Influence of the noise-expansion cascade on statistics*

Figure 6(a) compares time histories of the spatially averaged kinetic energy dissipation rate $\langle D\rangle_A$ of Flow CNS, Flow CNS′ and Flow CNS″, where $\langle\,\rangle_A$ is an operator of statistics defined in Appendix A. The distinct deviation in $\langle D\rangle_A$ between Flow CNS and Flow CNS′ appears at $t \approx 35$ when the evolution $\delta_1(x, y, t)$ of the first disturbance $10^{-20}\sin(x + y)$ increases to a macro-level $O(1)$ that finally destroys the spatial symmetry (3.1), and triggers the transformation of the spatial symmetry from (3.1) to (3.2). In addition, the distinct deviation in $\langle D\rangle_A$ of Flow CNS′ versus Flow CNS″ appears at $t \approx 93$ when the evolution $\delta_2(x, y, t)$ of the second disturbance $10^{-40}\sin(x + 2y)$ increases to a macro-level $O(1)$ that finally destroys all spatial symmetry. As shown in figure 6(a), when $t > 110$, the spatially averaged kinetic energy dissipation rate $\langle D\rangle_A$ of Flow CNS is much larger than the rates of Flow CNS′ and Flow CNS″. This leads to the obvious deviation between their probability density functions, as shown in figure 6(b). Figure 7 compares the spatiotemporal averaged kinetic energy $\langle E\rangle_{x,t}(y)$ and the spatiotemporal averaged kinetic energy dissipation rate $\langle D\rangle_{x,t}(y)$ of Flow CNS, Flow CNS′ and Flow CNS″, where $\langle\,\rangle_{x,t}$

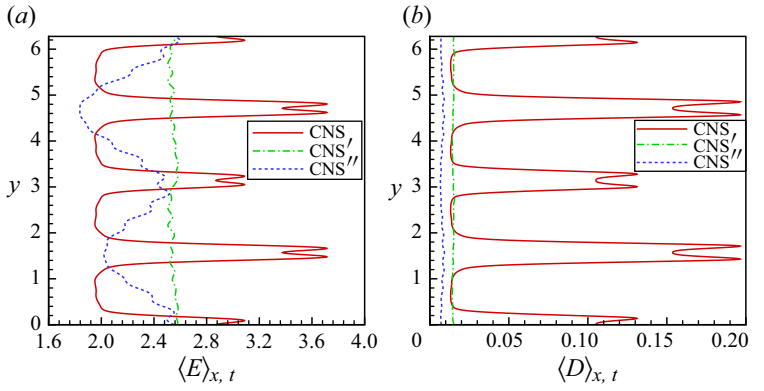

Figure 7. Comparisons of (*a*) the spatiotemporal averaged kinetic energy $\langle E\rangle_{x,t}(y)$ and (*b*) the spatiotemporal averaged kinetic energy dissipation rate $\langle D\rangle_{x,t}(y)$ of the 2-D turbulent Kolmogorov flow, governed by (2.1) and (2.2) for $n_K = 16$ and $Re = 2000$, given by Flow CNS subject to the initial condition (2.3) (red solid line), Flow CNS′ subject to the initial condition (3.3) (green dash-dotted line) and Flow CNS″ subject to the initial condition (3.4) (blue dashed line).

is an operator of statistics defined in Appendix A. Note that these statistics also exhibit obvious deviations.

The above results can be confirmed once again by comparing the kinetic energy spectra E_k of Flow CNS, Flow CNS′ and Flow CNS″, as shown in figure 8. When $t \in [0, 35]$, the deviations between the spatiotemporal trajectories of Flow CNS, Flow CNS′ and Flow CNS″ are negligible, and their corresponding kinetic energy spectra E_k agree quite well, as shown in figure 8(*a*) for $t = 30$. Thereafter, the evolution $\delta_1(x, y, t)$ of the first disturbance $10^{-20}\sin(x + y)$ increases to a macro-level $O(1)$ so that the kinetic energy spectra E_k of Flow CNS deviates from the spectra of Flow CNS′ and Flow CNS″ that remain the same until $t \approx 93$, as shown in figure 8(*b*) for $t = 80$. When the evolution $\delta_2(x, y, t)$ of the second disturbance $10^{-40}\sin(x + 2y)$ increases to a macro-level $O(1)$ at $t \approx 93$, all kinetic energy spectra E_k are different, as shown in figure 8(*c*) for $t = 130$. Note that all of them satisfy a $-5/3$ law, indicating that all of them are turbulent flows, no matter whether the vorticity field has spatial symmetry or not.

It is very interesting that Flow CNS contains more kinetic energy than Flow CNS′, and Flow CNS′ contains more kinetic energy than Flow CNS″, as shown in figure 8. This fact illustrates that turbulence with more spatial symmetries needs more kinetic energy to maintain. In order words, turbulence without spatial symmetry should be optimal from the viewpoint of energy. This is mainly because the spatially averaged kinetic energy dissipation rate $\langle D\rangle_A$ of Flow CNS is much larger than that of Flow CNS′, and the latter is larger than that of Flow CNS″, as shown in figure 6, indicating that turbulence with spatial symmetry indeed requires more kinetic energy to maintain. This might be the reason why turbulent flows have no spatial symmetry in practice.

Thus not only do all disturbances at different orders of magnitudes to the initial condition of the NS equations increase, one by one like an inverse cascade, to a macro level, but also each of them is capable of completely altering the macro-level characteristics of turbulent flow, even including certain statistical properties, as illustrated above. In other words, micro-level noise/disturbance might have great influence on macro-level characteristics and statistics of turbulence.

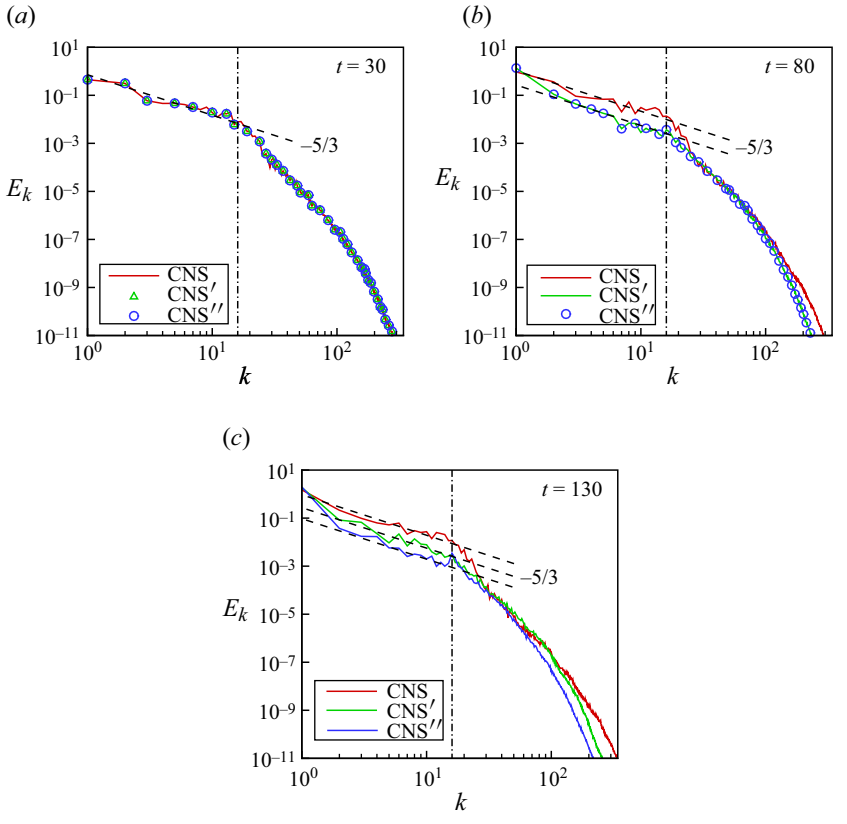

Figure 8. Kinetic energy spectra E_k of the 2-D turbulent Kolmogorov flow governed by (2.1) and (2.2) for $n_K = 16$ and $Re = 2000$ given by Flow CNS (red line), Flow CNS′ (green triangle or line) and Flow CNS″ (blue circle or line), at the different times (*a*) $t = 30$, (*b*) $t = 80$ and (*c*) $t = 130$, where a black dashed line corresponds to a $-5/3$ power law, and the black dash-dotted line denotes $k = n_K = 16$.

3.4. *An origin of randomness of turbulence*

The most surprising aspect of the noise-expansion cascade phenomenon is the fact that all disturbances, even if at quite different orders of magnitudes, separately enlarge to macro level, one by one like an inverse cascade. For example, for Flow CNS″ subject to the initial condition (3.4), the evolution $\delta_1(x, y, t)$ of the first disturbance $10^{-20}\sin(x + y)$ increases to macro level at $t \approx 35$, then triggers the transformation of the spatial symmetry of the flow field from (3.1) to (3.2), but the evolution $\delta_2(x, y, t)$ of the second disturbance $10^{-40}\sin(x + 2y)$ totally destroys the spatial symmetry of the turbulent flow when it increases to macro level at $t \approx 93$. This clearly indicates that the second disturbance $10^{-40}\sin(x + 2y)$ of the initial condition (3.4) can cause the turbulence characteristics (such as the vorticity spatial symmetry) to change greatly, even though the second disturbance is 20 orders of magnitude smaller than the first one. This strongly suggests that all disturbances must be considered for turbulence. This answers the second open question posed at the beginning of this paper.

Note that internal thermal fluctuation and external environmental disturbance are unavoidable in practice. In general, environmental disturbance is much larger than thermal fluctuation. So traditionally, thermal fluctuation is neglected for most turbulent flows, especially those governed by the NS equations. However, according to the noise-expansion

cascade concept proposed herein, thermal fluctuation must be considered for turbulence, even if it is many orders of magnitude smaller than environmental disturbance. Note that thermal fluctuation is essentially random, and this randomness can naturally transfer from the micro level to macro level through the noise-expansion cascade. This concept enables us to reveal an origin of randomness in turbulence, thus answering the first open question posed at the beginning of this paper.

4. Conclusion and discussion

Qin & Liao (2022) and Qin *et al.* (2024) recently demonstrated that the spatiotemporal trajectory given by direct numerical simulations (DNS) can rapidly become badly polluted by artificial numerical noise so that it becomes impossible for DNS to simulate accurately and rigorously the evolution and propagation of small disturbances in turbulent flow. Fortunately, clean numerical simulation (CNS) (Liao 2009; Liao & Wang 2014; Lin *et al.* 2017; Hu & Liao 2020; Qin & Liao 2020; Liao & Qin 2022; Qin & Liao 2023*a*,*b*, 2024) produces very much smaller artificial numerical noise than DNS, so can be used to provide clean numerical experiments for turbulence. In this paper, by means of a 'thought experiment' via several clean numerical experiments based on CNS for a 2-D turbulent Kolmogorov flow, it is discovered, for the first time, that all disturbances at different orders of magnitudes in initial condition of the NS equations quickly enlarge separately, one by one like an inverse cascade, to macro level. More importantly, each noise/disturbance might greatly change characteristics of the turbulent flow not only in the spatial symmetry of the flow, but also even in the statistics, thus clearly indicating that micro-level noise/disturbance might have great influence on macro-level characteristics and statistics of turbulence. Based on this interesting phenomenon, we propose a new concept, called the 'noise-expansion cascade', that closely connects the randomness of micro-level noise/disturbance to the macro-level disorder of turbulence. This reveals an origin of randomness in turbulence, thus answering the first open question posed at the beginning of the paper.

Note that internal thermal fluctuation and external environmental disturbance are unavoidable in practice. So according to the noise-expansion cascade, thermal fluctuation must be considered for turbulence, even if it is much smaller than external environmental disturbance, just as in the Landau–Lifshitz–Navier–Stokes equations that include the influence of thermal fluctuation (Landau & Lifshitz 1959). This answers the second open question that we mentioned at the beginning of this paper. Note that the influence of thermal fluctuation on turbulence has been recently reported by several researchers (Bandak *et al.* 2022; Ma *et al.* 2024).

Due to the noise-expansion cascade, many micro-level random factors might exert great influence on the macro-level disorder of turbulence. Hence the noise-expansion cascade should be viewed as a bridge connecting micro-level random fluctuation/disturbance to the macro-level disorder of turbulence. So the concept of the noise-expansion cascade provides a scientific explanation of the philosopher Heraclitus' aphorism that 'people cannot step twice into the same river'. It strongly implies that turbulence should be a unity of micro-level random noise/disturbance, their evolution and propagation, and macro-level disorder, which are closely connected through the noise-expansion cascade. This is why turbulence is so challenging to understand.

It should be emphasised that the noise-expansion cascade as a new concept cannot be discovered by numerical experiments based on DNS (since its artificial numerical noises increase exponentially) or physical experiments in the laboratory (since it is impossible in practice to have such accurate micro-level disturbances); this illustrates the great potential

of clean numerical experiments based on CNS. Note that the two micro-level disturbances $10^{-20}\sin(x+y)$ and $10^{-40}\sin(x+2y)$ hardly exist in practice; this is the reason why the noise-expansion cascade as a new fundamental concept of NS turbulence can be discovered only by such a 'thought experiment' based on CNS.

The noise-expansion cascade exhibits an obvious difference from the 'energy cascade' that is a fundamental concept in turbulence theory. There are two types of energy cascade: the direct energy cascade whereby energy transfers from large scale to small scale; and the inverse energy cascade whereby energy transfers from small scale to large scale. However, unlike the energy cascade, the noise-expansion cascade has only one direction: from micro scale to large scale. Moreover, the energy cascade describes spatial transfer of energy, whereas the noise-expansion cascade describes the temporal evolution and propagation of initial noise/disturbance. Recently, it was reported that the average uncertainty energy of NS turbulence grows exponentially (Aurell *et al.* 1996; Boffetta & Musacchio 2001; Boffetta & Boffetta & Ecke 2012; Lin *et al.* 2017; Ge *et al.* 2023; Ma *et al.* 2024). This phenomenon, sometimes called 'inverse error cascade', is observed using different initial conditions at the same order of magnitude. However, the noise-expansion cascade focuses on the influence of initial conditions with different orders of magnitude. This further underlines the novelty of the noise-expansion cascade as a new fundamental concept of NS turbulence.

At each time step, the DNS algorithm unavoidably contains artificial numerical noise. Thus due to the noise-expansion cascade, the artificial numerical noise of the DNS algorithm at each time step will increase consistently to reach the macro level: this is exactly why the spatiotemporal trajectory of DNS departs quickly from the true solution, and why the noise-expansion cascade cannot be revealed by DNS.

Actually, CNS requires substantial computer resources and is time-consuming to run at present, just like DNS when Orszag (1970) proposed it. For the 2-D turbulent Kolmogorov flow under consideration, the parallel computing of the CNS takes 285 hours (i.e. approximately 12 days) using 4096 CPUs (Intel's CPU: Xeon Gold 6348, 2.60 GHz) of the Tian-He New Generation Supercomputer at the National Supercomputer Center in Tianjin, China. The related code of CNS and some movies can be downloaded via GitHub (https://github.com/sjtu-liao/2D-Kolmogorov-turbulence). By contrast, DNS of the same case require only 13 hours using 1024 CPUs on the same computing platform. Even so, CNS undoubtedly provides us with a new way to investigate turbulence through clean numerical experiments, i.e. with negligible artificial numerical noise, as illustrated in this paper.

We would like to emphasise that DNS is a milestone in fluid mechanics, since it opened a new era of numerical experiment and has greatly promoted the progress of turbulence in theories, physical experiments and applications. In essence, CNS can be regarded as a general form of DNS with rigorously negligible numerical noise in a finite but long enough time interval $t \in [0, T_c]$, where T_c is the so-called 'critical predictable time'. In other words, the critical predictable time T_c of CNS is much longer than that of DNS. Thus CNS offers a powerful method by which to accurately investigate the influence of micro-scale physical/artificial disturbances on macro-scale characteristics and statistics of turbulent flow.

Note that, like DNS, CNS has 'the ability to perform fundamental studies of *clean* flows *unaffected* by numerical, modelling and measurement errors' and 'the complete control of the initial and boundary conditions, and each term in the governing equations, also leads to profound advantages over laboratory and field studies' (Coleman & Sandberg 2010). It is found that our conclusions are qualitatively same as those mentioned above even if we use the different first disturbance such as $10^{-10}\sin(x+y)$ and the different second

disturbance such as $10^{-20}\sin(x+2y)$. We emphasise that it is impossible to accurately have such kinds of micro-level disturbances at quite different orders of magnitude by physical experiments in a laboratory, thus we in fact did a thought experiment of the NS turbulence by means of CNS in this paper. Note that it is this thought experiment that reveals the new fundamental concept 'noise-expansion cascade'. Here, we emphasise once again that the noise-expansion cascade not only reveals an origin of randomness of turbulence, but also highly indicates that micro-level noises/disturbances might have great influence on macro-level characteristics and statistics of turbulence. In other words, macro-level characteristics and statistics of turbulence should be determined not only by its spatial domain of flow and its initial/boundary conditions, but also by its micro-level noises/disturbances. We hope that the noise-expansion cascade as a fundamental property of the NS equations could greatly deepen our understandings about turbulence, and is also helpful for attacking the fourth millennium problem posed by the Clay Mathematics Institute of Cambridge, Massachusetts (2000).

There are many interesting problems worthy of further investigation in future. For example, it might be possible that artificial numerical noise could be regarded as a kind of physical external disturbance, as long as we could prove that artificial numerical noise could have the same influences as thermal fluctuation and/or environmental disturbance to turbulent flow, which unfortunately is still an open question up to now. This kind of investigation might reveal the essence of artificial numerical noises to turbulent flow. In addition, thermal fluctuation is random and discontinuous, but it is still an open question whether or not such discontinuous random disturbance might become continuous when it increases to macro level due to the noise-expansion cascade. In particular, there exist two types of chaotic system, i.e. normal chaos and ultra chaos (Liao & Qin 2022); unlike normal chaos, statistics of ultra chaos are unstable (or sensitive) to small disturbances (Qin & Liao 2023*a*; Yang *et al.* 2023*a*,*b*; Zhang & Liao 2023; Zhang, Yang & Liao 2024; Yang & Liao 2024). In other words, statistical non-reproducibility is an inherent property of an ultra chaos, so that an ultra chaos is at a higher level of disorder than a normal chaos. If a turbulent flow belongs to an ultra chaos, say, its statistics are sensitive (i.e. unstable) to small noise/disturbance, then due to the noise-expansion cascade, its statistics are unstable/sensitive to physical environmental disturbances or artificial numerical noises so that statistical reproducibility of experimental/numerical results does not exist. However, it is an open question how to solve (or understand) sucha kind of ultra-chaotic turbulence without reproducibility of statistics.

Supplementary material. Supplementary material are available at https://doi.org/10.1017/jfm.2025.140.

Acknowledgements. Thanks to the anonymous reviewers for their valuable suggestions and constructive comments. The calculations were performed on the Tian-He New Generation Supercomputer, National Supercomputer Center in Tianjing, China.

Funding. This work is supported by State Key Laboratory of Ocean Engineering, Shanghai 200240, China.

Declaration of interests. The authors report no conflict of interest.

Author contributions. S.L. conceived/designed the numerical experiments, proposed the new concept 'noise-expansion cascade', and wrote the manuscript. S.Q. performed the numerical simulation and plotted the figures.

Data availability statement. The data that support the findings of this study are available on request from the corresponding author. In addition, the related code of CNS and some movies can be downloaded via GitHub (https://github.com/sjtu-liao/2D-Kolmogorov-turbulence).

Appendix A. Some definitions and measures

For simplicity, the definitions of some statistical operators are briefly described below. The operator of spatial average is defined by

$$\langle f \rangle_A = \frac{1}{4\pi^2} \int_0^{2\pi} \int_0^{2\pi} f \, \mathrm{d}x \, \mathrm{d}y, \tag{A1}$$

and the operator of spatiotemporal average (along the x direction) is defined by

$$\langle f \rangle_{x,t} = \frac{1}{2\pi(T_2 - T_1)} \int_0^{2\pi} \int_{T_1}^{T_2} f \, \mathrm{d}x \, \mathrm{d}t, \tag{A2}$$

where $T_1 = 100$ (for Flow CNS and Flow CNS$'$) or 120 (for Flow CNS$''$) and $T_2 = 300$ are used in this paper to calculate statistics.

The kinetic energy is given by

$$E(x, y, t) = \tfrac{1}{2}\big[u^2(x, y, t) + v^2(x, y, t)\big], \tag{A3}$$

and the kinetic energy dissipation rate is defined by

$$D(x, y, t) = \frac{1}{2\,Re} \sum_{i,j=1,2} \big[\partial_i u_j(x, y, t) + \partial_j u_i(x, y, t)\big]^2, \tag{A4}$$

where $u_1(x, y, t) = u(x, y, t)$, $u_2(x, y, t) = v(x, y, t)$, $\partial_1 = \partial/\partial x$ and $\partial_2 = \partial/\partial y$.

The stream function can be expanded as the Fourier series

$$\psi(x, y, t) \approx \sum_{m=-\lfloor N/3 \rfloor}^{\lfloor N/3 \rfloor} \sum_{n=-\lfloor N/3 \rfloor}^{\lfloor N/3 \rfloor} \Psi_{m,n}(t) \exp(\mathrm{i}mx) \exp(\mathrm{i}ny), \tag{A5}$$

where m, n are integers, $\lfloor\ \rfloor$ stands for a floor function, $\mathrm{i} = \sqrt{-1}$ denotes the imaginary unit, and for dealiasing $\Psi_{m,n} = 0$ is imposed for wavenumbers outside the above domain $\sum$. Note that for the real number ψ, $\Psi_{-m,-n} = \Psi^*_{m,n}$ must be satisfied, where $\Psi^*_{m,n}$ is the conjugate of $\Psi_{m,n}$. Therefore, the kinetic energy spectrum is defined as

$$E_k(t) = \sum_{k-1/2 \leqslant \sqrt{m^2+n^2} < k+1/2} \tfrac{1}{2}(m^2 + n^2)\, |\Psi_{m,n}(t)|^2, \tag{A6}$$

where the wavenumber k is a non-negative integer.

References

Alexakis, A., Marino, R., Mininni, P.D., van Kan, A., Foldes, R. & Feraco, F. 2024 Large-scale self-organization in dry turbulent atmospheres. *Science* **383** (6686), 1005–1009.

Aurell, E., Boffetta, G., Crisanti, A., Paladin, G. & Vulpiani, A. 1996 Growth of noninfinitesimal perturbations in turbulence. *Phys. Rev. Lett.* **77** (7), 1262–1265.

Bandak, D., Goldenfeld, N., Mailybaev, A.A. & Eyink, G. 2022 Dissipation-range fluid turbulence and thermal noise. *Phys. Rev.* E **105** (6), 065113.

Berera, A. & Ho, R.D. J G. 2018 Chaotic properties of a turbulent isotropic fluid. *Phys. Rev. Lett.* **120** (2), 024101.

Boffetta, G. & Ecke, R.E. 2012 Two-dimensional turbulence. *Annu. Rev. Fluid Mech.* **44**, 427–451.

Boffetta, G. & Musacchio, S. 2001 Predictability of the inverse energy cascade in 2D turbulence. *Phys. Fluids* **13** (4), 1060–1062.

Boffetta, G. & Musacchio, S. 2010 Evidence for the double cascade scenario in two-dimensional turbulence. *Phys. Rev.* E **82** (1), 016307.

BOFFETTA, G. & MUSACCHIO, S. 2017 Chaos and predictability of homogeneous-isotropic turbulence. *Phys. Rev. Lett.* **119** (5), 054102.
CHANDLER, G.J. & KERSWELL, R.R. 2013 Invariant recurrent solutions embedded in a turbulent two-dimensional Kolmogorov flow. *J. Fluid Mech.* **722**, 554–595.
Clay Mathematics Institute of Cambridge, Massachusetts. 2000 The Millennium Prize Problems. https://www.claymath.org/millennium-problems/
COLEMAN, G.N. & SANDBERG, R.D. 2010 A primer on direct numerical simulation of turbulence – methods, procedures and guidelines. Tech. Rep. AFM-09/01a. Aerodynamics & Flight Mechanics Research Group, University of Southampton, UK.
CRANE, L. 2017 *Infamous three-body problem has over a thousand new solutions*. New Scientist
DAVIDSON, P.A. 2004 *Turbulence: An Introduction for Scientists and Engineers*. Oxford University Press.
DEISSLER, R.G. 1986 Is Navier–Stokes turbulence chaotic? *Phys. Fluids* **29** (5), 1453–1457.
GE, J., ROLLAND, J. & VASSILICOS, J.C. 2023 The production of uncertainty in three-dimensional Navier–Stokes turbulence. *J. Fluid Mech.* **977**, A17.
HU, T. & LIAO, S. 2020 On the risks of using double precision in numerical simulations of spatio-temporal chaos. *J. Comput. Phys.* **418**, 109629.
LANDAU, L.D. & LIFSHITZ, E.M. 1959 *Course of Theoretical Physics: Fluid Mechanics*. Vol. 6. Addison-Wesley.
LI, X., JING, Y. & LIAO, S. 2018 Over a thousand new periodic orbits of a planar three-body system with unequal masses. *Publ. Astron. Soc. Japan* **70** (4), 64.
LI, X. & LIAO, S. 2017 More than six hundred new families of Newtonian periodic planar collisionless three-body orbits. *Sci. China Phys. Mech. Astron.* **60** (12), 129511.
LIAO, S. 2009 On the reliability of computed chaotic solutions of non-linear differential equations. *Tellus Ser. A: Dyn. Meteorol. Oceanol.* **61** (4), 550–564.
LIAO, S. 2023 *Clean Numerical Simulation*. Chapman and Hall/CRC.
LIAO, S., LI, X. & YANG, Y. 2022 Three-body problem – from Newton to supercomputer plus machine learning. *New Astron.* **96**, 101850.
LIAO, S. & QIN, S. 2022 Ultra-chaos: an insurmountable objective obstacle of reproducibility and replication. *Adv. Appl. Maths Mech.* **14** (4), 799–815.
LIAO, S. & WANG, P. 2014 On the mathematically reliable long-term simulation of chaotic solutions of Lorenz equation in the interval [0, 10000]. *Sci. China Phys. Mech. Astron.* **57** (2), 330–335.
LIN, Z.L., WANG, L.P., & LIAO, S.J. 2017 On the origin of intrinsic randomness of Rayleigh–Bénard turbulence. *Sci. China Phys. Mech. Astron.* **60** (1), 1–13.
MA, Q., YANG, C., CHEN, S., FENG, K., CUI, Z. & ZHANG, J. 2024 Effect of thermal fluctuations on spectra and predictability in compressible decaying isotropic turbulence. *J. Fluid Mech.* **987**, A29.
NELKIN, M. 1992 In what sense is turbulence an unsolved problem? *Science* **255** (5044), 566–570.
OBUKHOV, A.M. 1983 Kolmogorov flow and laboratory simulation of it. *Russian Math. Surv.* **38** (4), 113–126.
ORSZAG, S.A. 1970 Analytical theories of turbulence. *J. Fluid Mech.* **41** (2), 363–386.
OYANARTE, P. 1990 MP – a multiple precision package. *Comput. Phys. Commun.* **59** (2), 345–358.
POPE, S.B. 2001 *Turbulent Flows*. IOP Publishing.
QIN, S. & LIAO, S. 2020 Influence of numerical noises on computer-generated simulation of spatio-temporal chaos. *Chaos, Solitons Fractals* **136**, 109790.
QIN, S. & LIAO, S. 2022 Large-scale influence of numerical noises as artificial stochastic disturbances on a sustained turbulence. *J. Fluid Mech.* **948**, A7.
QIN, S. & LIAO, S. 2023*a* A kind of Lagrangian chaotic property of the Arnold–Beltrami–Childress flow. *J. Fluid Mech.* **960**, A15.
QIN, S. & LIAO, S. 2023*b* A self-adaptive algorithm of the clean numerical simulation (CNS) for chaos. *Adv. Appl. Maths Mech.* **15** (5), 1191–1215.
QIN, S. & LIAO, S. 2024 Influences of artificial numerical noise on statistics and qualitative properties of chaotic system. *Physica* D **470**, 134355.
QIN, S., YANG, Y., HUANG, Y., MEI, X., WANG, L. & LIAO, S. 2024 Is a direct numerical simulation (DNS) of Navier–Stokes equations with small enough grid spacing and time-step definitely reliable/correct? *J. Ocean Engng Sci.* **9** (3), 293–310.
ROGALLO, R.S. 1981 Numerical experiments in homogeneous turbulence. Tech. Rep. NASA-TM-81315, NASA, USA.
SHE, Z.-S., JACKSON, E. & ORSZAG, S.A. 1990 Intermittent vortex structures in homogeneous isotropic turbulence. *Nature* **344** (6263), 226–228.
WHYTE, C. 2018 *Watch the weird new solutions to the baffling three-body problem*. New Scientist

WU, W., SCHMITT, F.G., CALZAVARINI, E. & WANG, L. 2021 A quadratic Reynolds stress development for the turbulent Kolmogorov flow. *Phys. Fluids* **33** (12), 125129.

YANG, Y. & LIAO, S. 2024 Ultra-chaos: a great challenge for machine learning and AI. *Intl J. Bifurcation Chaos* **34** (16), 2450202.

YANG, Y., QIN, S. & LI, S. 2023*a* Ultra-chaos in the motion of walking droplet. *Intl J. Bifurcation Chaos* **33** (16), 2350191.

YANG, Y., QIN, S. & LIAO, S. 2023*b* Ultra-chaos of a mobile robot: a higher disorder than normal-chaos. *Chaos, Solitons Fractals* **167**, 113037.

ZHANG, B. & LIAO, S. 2023 Ultra-chaos in a meandering jet flow. *Physica* D **455**, 133886.

ZHANG, B., YANG, Y. & LIAO, S. 2024 Ultra-chaos of square thin plate in low Earth orbit. *Acta Mechanica Sin.* **40** (5), 523428.